Ocean and Coastal Management 217 (2022) 106009

Contents lists available at ScienceDirect

Ocean and Coastal Management

journal homepage: www.elsevier.com/locate/ocecoaman

Model-based estimation of plastic debris accumulation in Banten Bay, Indonesia, using particle tracking - Flow model hydrodynamics approach

Ulung J. Wisha [a,b,*], Wisnu A. Gemilang [a], Yusuf J. Wijaya [b,c], Anang D. Purwanto [d]

[a] Research Institute for Coastal Resources and Vulnerability, Ministry of Marine Affairs and Fisheries, Padang, Sumatra Barat, 25245, Indonesia
[b] Department of Physics and Earth Sciences, Faculty of Science, University of the Ryukyus, Nishihara, Okinawa, 903-0213, Japan
[c] Department of Oceanography, Faculty of Fisheries and Marine Science, Diponegoro University, Semarang, Jawa Tengah, 50175, Indonesia
[d] Remote Sensing Application Center, National Research and Innovation Agency (BRIN), Jakarta, 13710, Indonesia

ARTICLE INFO

Keywords:
Plastic debris pollution
Hydrodynamic simulation
Semi-enclosed waters
Coastal cleanup

ABSTRACT

Coastal pollution caused by marine debris in Banten Bay is increasing and threatening the environmental and ecological sustainability of the bay's coastal area. This study aims to simulate the particle tracking of floating plastic debris within Banten Bay and to estimate the coastal debris accumulation for the period 2018 to 2028 based on numerical spatial modeling. To determine the dominant direction of plastic debris flow, we recorded floating plastic waste at four locations (Bojonegara port, Karangantu Estuary, Cibanten Estuary, and the Sunda Straits) by releasing wooden drifters. The numerical model was developed using a Particle Tracking module based on the Langevin equation. In comparison to data provided by the drifter survey, the particle tracking showed a similar distribution trace that tended to move westward during the northeast monsoon and eastward during the southwest monsoon. During the northeast monsoon, marine debris intake peaked, ranging from 2.25 kg to 5.75 kg. We estimated that over the ten years modeled plastic debris accumulation would increase by approximately 11%, to a maximum rate of 9.42 kg/day. Of particular concern, it is modeled that 41% of Banten Bay will be covered by plastic debris in 2028 if effective mitigations are not immediately applied. We recommend conducting a coastal cleanup operation every ten days so that coastal debris deposits can be well-controlled.

1. Introduction

Marine pollution is an issue of concern, with many reports indicating that the level of pollution is rapidly increasing, resulting in environmental degradation and economic losses (Inniss and Simcock, 2017). Marine debris pollution is the primary factor threatening marine ecosystems and hampering biota survival (Potocka et al., 2019). Much online news reports that the enormous amount of floating plastic debris has started to impact on living biota, for example, sperm whales (*Physeter Macrocephalus*) dying as a result of plastics in their digestive tracks in Wakatobi, Indonesia (Mahbub, 2018). Several studies have also reported various marine biota ingesting and becoming entangled in plastic litters (Lebreton et al., 2012; Van Sebille et al., 2012).

As economies grow rapidly, use of plastic will continue to increase, resulting in accumulated plastic debris in the marine environment (Van Sebille et al., 2012). As a developing country, Indonesia's use of plastics has increased tremendously, and much of the plastic waste from this use will accumulate in the country's waters. As a result, the UN environment program names Indonesia as one of the main contributors to marine debris (Purba et al., 2019). The Indonesia archipelago is an area of significance because of its geographical location, positioned as it is between two continents and oceans and contributing to the inter-ocean and anthropogenic-sourced debris intakes. One of the impacted regions is Banten Bay, with its dense human population being a main factor in the substantial scale of marine debris seasonally accumulated in and polluting the Banten coastal bay.

Banten Bay is a semi-enclosed area of water situated in the Banten Province, Indonesia. It is surrounded by Serang Regency and Serang City and has a bathymetry profile ranging from 0 to 40 m beneath sea level (Fig. 1a). It has been designated a protected marine conservation area both because it contains several historical remains from World War II (*USS Houston* and *HMAS Perth* shipwrecks) and because it supports very high biodiversity. In its location close to the Sunda Strait, which contributes the gateway to the Indonesian Throughflow (ITF), Banten Bay is

* Corresponding author. Research Institute for Coastal Resources and Vulnerability, Ministry of Marine Affairs and Fisheries, Padang, Sumatra Barat, 25245, Indonesia.

E-mail address: ulungjantama@kkp.go.id (U.J. Wisha).

https://doi.org/10.1016/j.ocecoaman.2021.106009
Received 17 October 2021; Received in revised form 8 December 2021; Accepted 8 December 2021
0964-5691/© 2021 Elsevier Ltd. All rights reserved.

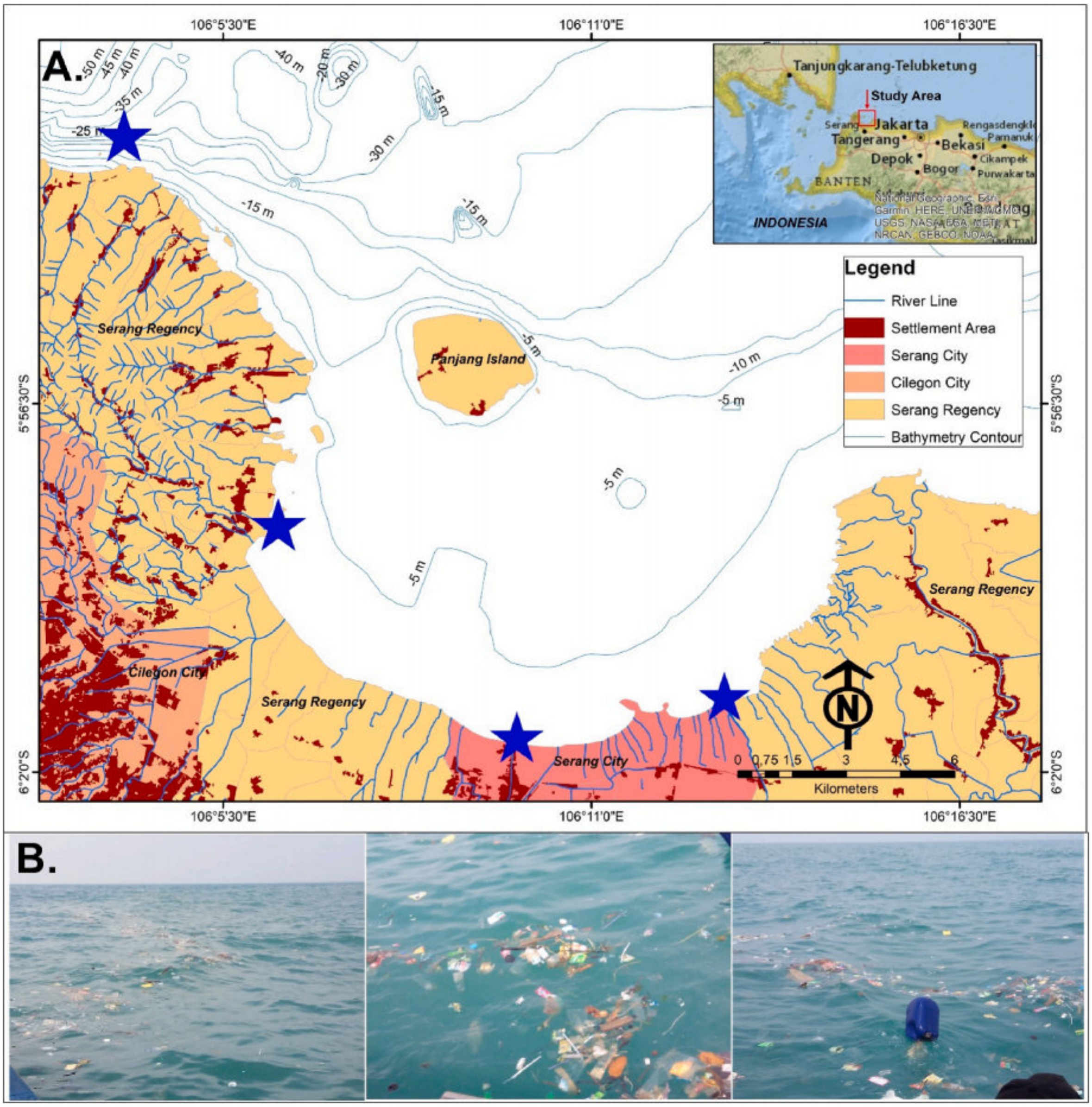

Fig. 1. The study area (a) and seasonal marine debris documentation within Banten Bay (b). Blue stars denote the main source of marine debris. (Source: on-screen digitation of Google Earth image and field survey in 2018). (For interpretation of the references to color in this figure legend, the reader is referred to the Web version of this article.)

frequently influenced by inter-ocean pollution (Susanto et al., 2016). The connection between the Indian and the Pacific Oceans through Indonesia's seas such as the Sunda Strait plays a significant role in accumulating marine debris (Husrin et al., 2017) via the transit area of debris fragments, thereby hampering the ecosystems within the bay. Additionally, the areas of settlement concentrated on surrounding riverbanks allow large amounts of anthropogenic solid waste to flow into the bay via river runoff. (Fig. 1a).

The most dangerous pollutants within Banten Bay are plastics and other non-degradable materials sourced from anthropogenic activities. These include dumped waste, littering from tourism, waste from shipping, and fishery industries (Werner et al., 2016). The movement of marine debris depends on the tidal current flows that play a significant role in the transport mechanisms within the bay (Wisha et al., 2015). Particles will move landward during high tides and will circulate around the mouth of the bay during ebb tides. The floating marine debris in the bay consists largely of plastic fragments, jerrycans, polyethylene packaging, twigs, plastic and glass bottles, cigarettes, sanitary pads, and other solid particles (Fig. 1b). As a semi-enclosed water area, hydrodynamics within Banten Bay tends to be weak (Bayhaqi et al., 2018), potentially causing higher debris accumulation within the bay.

Monsoon-induced movement of water mass triggers marine debris distribution within Banten Bay (Maharani et al., 2018). Rahmania et al. (2021) report that the solid waste volume increased sixfold over 22 years (1995–2017), with higher accumulation occurring during rainy seasons. Consequently, pollution by plastic fragments in Banten Bay is greatly elevated (Rifa'i, 2018). One way to determine the propagation of plastic fragments is via a numerical model approach based on particle tracking simulation. This method enables us to delineate the likely actual conditions when the field surveys cannot fully cover the study area.

The particle tracking model has been widely used to determine the distribution of marine debris worldwide (Lebreton et al., 2012; Liubartseva et al., 2016; Miladinova et al., 2020; Potemra, 2012). In Indonesian waters, an associated flow version is commonly used for determining sediment particle distribution. However, this approach has

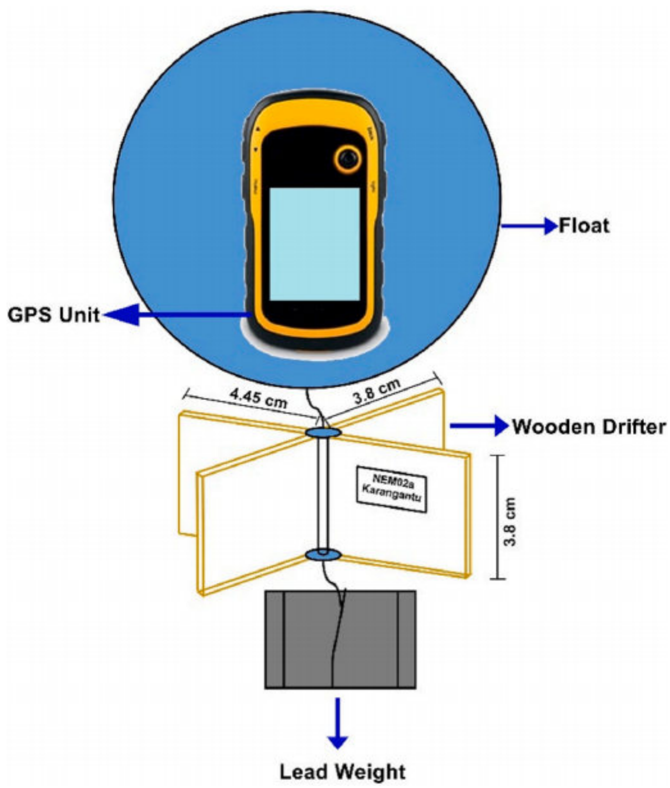

Fig. 2. The design of wooden drifter used during field survey in Banten Bay.

rarely been used for estimating marine debris trajectories (Husrin et al., 2017; Rahmania et al., 2021). As to date there are no reports predicting long-term debris distribution and pollution in Banten Bay, this topic will be investigated in this study. The study will develop a flexible mesh flow model to simulate the tracking of debris particles with various fragment masses validated by a field drifter survey. It is expected to create a model-based estimation of marine debris accumulation throughout the Banten Bay coastline over a ten-year period (2018–2028) as a basis for future decision-making regarding marine debris pollution in Banten Province. This study aims to determine the dominant form of propagation of floating plastic fragments and to estimate the debris accumulation rate in Banten Bay.

2. Materials and methods

2.1. Field survey using floating drifter drogue

We chose three sources of marine debris within Banten Bay (the port of Bojonegara, Karangantu Estuary, and Cibanten Estuary) and another source in the Sunda Strait (Fig. 1). We chose these four sources based on results obtained from a preliminary field survey identifying locations where many debris fragments were visually observed. We deployed degradable wooden drifters to predict the movement of Banten Bay-sourced debris. Each drifter was 7.6 cm in length, 8.9 cm in width, and 3.8 cm in height and branded with a message including release location code, the tidal condition on release, and contact phone number. We tracked the drifters by deploying GPS receiver Garmin eTrex 10 010-00970-00 model along with them to monitor their movement paths (Fig. 2). We released eight groups of drifters at the four sources (Sunda Strait, Bojonegara port, Karangantu Estuary, and Cibanten Estuary) (Fig. 2) in two deployments, one in January 2018 and another in June 2018. We released drifters twice in consideration of tidal conditions at slack-before-flood and slack-before-ebb (Table 1). We released a total of 16 wooden drifters at the four points. The results of this survey provided data against which we could validate the particle tracking model simulated in this study.

From those chosen sources we also trapped the fragmental debris using a net deployed from a boat along the estuaries. This survey was conducted monthly during the spring tides throughout 2018 when the peak production of anthropogenic debris was expected. Rainfall intensity is crucial in inducing higher debris intake to the bay through surface runoff (Silva et al., 2016) and we therefore mounted a portable automatic weather station to record the daily rainfall-induced surface runoff.

2.2. Development of hydrodynamic and particle tracking equations

A particle tracking technique is an efficient way to predict the fate of matter in the waters. The basic principle of this technique considers the drift regime components such as longshore currents in the transport particles (Miladinova et al., 2020). In this study, we employed the Particle Tracking module of MIKE 21 Flow Model FM to model plastic debris trajectories within Banten Bay with a spatial analysis approach to depict the model results. The hydrodynamic basis applied in the particle tracking module was simulated beforehand using the hydrodynamic module within the Flow Model FM modeling system. The flow model is based on the 3D incompressible Reynolds-averaged Navier-Stokes equations, applying the local continuity and the two horizontal momentum equations for x and y components (Zhao et al., 1994) as follows:

$$\frac{\partial u}{\partial x}+\frac{\partial v}{\partial y}+\frac{\partial w}{\partial z}=S \tag{1}$$

$$\frac{\partial u}{\partial t}+\frac{\partial u^2}{\partial x}+\frac{\partial vu}{\partial y}+\frac{\partial wu}{\partial z}=fv-g\frac{\partial \eta}{\partial x}-\frac{1}{\rho_o}\frac{\partial P_a}{\partial x}-\frac{g}{\rho_o}\int_z^{\eta}\frac{\partial \rho}{\partial x}dz-\frac{1}{\rho_o h}\left(\frac{\partial S_{xx}}{\partial x}+\frac{\partial S_{xy}}{\partial y}\right)+F_u+\frac{\partial}{\partial z}\left(V_t\frac{\partial u}{\partial z}\right)+U_sS \tag{2}$$

$$\frac{\partial v}{\partial t}+\frac{\partial v^2}{\partial y}+\frac{\partial uv}{\partial x}+\frac{\partial wv}{\partial z}=-fu-g\frac{\partial \eta}{\partial y}-\frac{1}{\rho_o}\frac{\partial P_a}{\partial y}-\frac{g}{\rho_o}\int_z^{\eta}\frac{\partial \rho}{\partial y}dz-\frac{1}{\rho_o h}\left(\frac{\partial S_{yx}}{\partial x}+\frac{\partial S_{yy}}{\partial y}\right)+F_v+\frac{\partial}{\partial z}\left(V_t\frac{\partial v}{\partial z}\right)+V_sS \tag{3}$$

Table 1
Wooden-drifter releases at the four source points.

Location	Tidal condition	Code	Date
Bojonegara Port 1	Ebb tides	NEM01a	January 24th, 2018
	Flood tides	NEM01b	
Karangantu 1	Ebb tides	NEM02a	January 25th, 2018
	Flood tides	NEM02b	
Cibanten 1	Ebb tides	NEM03a	January 26th, 2018
	Flood tides	NEM03b	
Sunda Strait 1	Ebb tides	NEM04a	January 27th, 2018
	Flood tides	NEM04b	
Bojonegara Port 2	Ebb tides	SW01a	June 15th, 2018
	Flood tides	SW01b	
Karangantu 2	Ebb tides	SW02a	June 16th, 2018
	Flood tides	SW02b	
Cibanten 2	Ebb tides	SW03a	June 17th, 2018
	Flood tides	SW03b	
Sunda Strait 2	Ebb tides	SW04a	June 18th, 2018
	Flood tides	SW04b	

where:

t = Time
x, y, z = Cartesian coordinate
η = Water level
d = Still water depth
h = Total water depth ($h = \eta + d$)
u, v, w = Velocity components in the x, y, and z directions
$f = 2\Omega sin\varphi$ (Coriolis parameter)
g = Specific gravity
ρ = Density
$S_{xx}, S_{xy}, S_{yx}, S_{yy}$ = Components of radiation stress tensor
vt = Vertical turbulent (eddy viscosity)
Pa = Atmospheric pressure
ρo = Reference density
S = Magnitude of discharge from point sources
(U_s, V_s) = Velocity when the condition of the water is discharged into ambient water
F_u, F_v = Horizontal stress terms, elucidated using a gradient-stress relation; $F_u = \frac{\partial}{\partial x}\left(2A\frac{\partial u}{\partial x}\right) + \frac{\partial}{\partial y}\left(A\left(\frac{\partial u}{\partial y}+\frac{\partial v}{\partial x}\right)\right)$ and $F_v = \frac{\partial}{\partial x}\left(A\left(\frac{\partial u}{\partial y}+\frac{\partial v}{\partial x}\right)\right) + \frac{\partial}{\partial y}\left(2A\frac{\partial v}{\partial y}\right)$ with A is the horizontal eddy viscosity.

The surface and bottom boundary conditions for u, v and w are described as follows:

At $z = \eta$:

$$\frac{\partial \eta}{\partial t} + u\frac{\partial \eta}{\partial x} + v\frac{\partial \eta}{\partial y} - w = 0,\ \left(\frac{\partial u}{\partial z}, \frac{\partial v}{\partial z}\right) = \frac{1}{\rho_{0V_t}}(\tau_{sx}, \tau_{sy}) \tag{4}$$

At $z = -d$:

$$u\frac{\partial d}{\partial x} + v\frac{\partial d}{\partial y} + w = 0,\ \left(\frac{\partial u}{\partial z}, \frac{\partial v}{\partial z}\right) = \frac{1}{\rho_{0V_t}}(\tau_{bx}, \tau_{by}) \tag{5}$$

where:

(τ_{sx}, τ_{sy}) = the x and y component of the surface winds
(τ_{bx}, τ_{by}) = the x and y component of the bottom stresses

The particle tracking model applied a Lagrangian discrete parcel method that disregarded the interaction between diffusing particles (Ouellette et al., 2006). We assumed that particles would be subject to velocity transfers from water mass movement for instant acceleration. In considering particle mass, zero-mass particle error was not substantial, while error would be significant if the particles were large (North et al., 2008). Moreover, the particle tracking technique describing transport and dispersion of particles followed the Langevin equation to formulate these motion dynamics in terms of stochastic differential equations (Bayram et al., 2018) as follows:

$$dX_t = a(t, X_t)dt + b(t, X_t)\xi_t dt \tag{6}$$

where:

a = Drift term
b = Diffusion term
ξ = Random number

To simulate a trajectory, we discretized the Euler estimation Y for a given time from the initial value of $Y_o = X_o$; then it yielded formula as follows:

$$Y_{n+1} = Y_n + a(t, X_t)Y_n\Delta_n + b(t, X_t)Y_n\Delta W_n \tag{7}$$

$$\Delta W_n = W_t - W_s \in N\left(\mu = 0, \sigma^2 = \Delta_n\right) \tag{8}$$

where:

n = 1,2,3, …according to the Euler scheme with drift a and diffusion coefficient b
ΔW_n = Normal distributed Gaussian increment of the Wiener process W,
W = a continuous-time Gaussian stochastic process with independent increments over the subinterval $\tau_n \le t \le \tau_{n+1}$

In this simulation, particles were divided into different classes with specific properties specified separately, such as decay, settling/buoyancy, erosion, and dispersion. Furthermore, we also determined a minimum mass and maximum age of particle, but we did not consider the decay process for marine debris particles because inorganic matter decay was impossible to include in the simulation.

The drift term of the particles caused by the combined effects of current and wind drag causing advection of particles is described as follows:

$$\vec{a}(x, y, z, t) = f(current, wind\ drag) \tag{9}$$

The horizontal variation in the drift vector is yielded from the hydrodynamic simulation. However, as the wind-driven current occurs, the bed resistance factors will not impact the flow pattern. The horizontal drift variation could be estimated directly as the wind function by considering Ekman spiral theory, as follows:

$$U_E = \pm\ 0.79.10^{-5}\frac{W^2}{D_E|f|_o}cos\left(\frac{\pi}{4}+\frac{\pi}{D_E}z\right)exp\left(\frac{\pi}{D_E}z\right) \tag{10}$$

$$V_E = \pm\ 0.79.10^{-5}\frac{W^2}{D_E|f|}sin\left(\frac{\pi}{4}+\frac{\pi}{D_E}z\right)exp\left(\frac{\pi}{D_E}z\right) \tag{11a}$$

where:

V_o = Ekman surface current $V_o = 0.79.10^{-5}\frac{W^2}{D_E|f|}$
D_E = Ekman depth, or depth of frictional influence
f=$2\Omega sin\varphi$ (Coriolis parameter)
Ω = Angular velocity of the earth $\Omega = 7.29.\ 10^{-5}\frac{rad}{s}$
φ = Latitude

Wind-exposed particles on the surface are affected by the wind regimes in two ways: either indirectly through the currents including wind, or as an extra force directly on the particle (Neumann et al., 2014). The effect of these two wind regimes depends on the particle's nature determining the characteristics of the wind-exposed particle. In the simulation, the wind acceleration of surface particles affected the drift with the following modification:

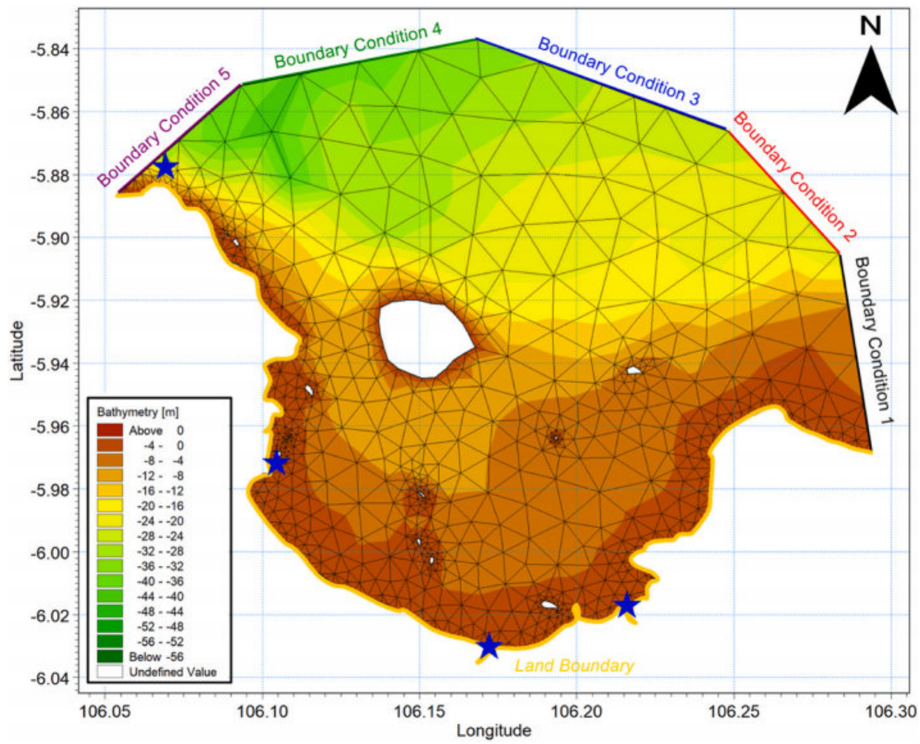

Fig. 3. The study and simulation area consisted of a mesh file (mesh triangulation and boundary conditions) and the position of sources (blue stars) applied in the model. (For interpretation of the references to color in this figure legend, the reader is referred to the Web version of this article.)

$$\theta_w = \beta exp exp\left(\frac{-0.3.10^{-9}|U_w|^{28^o 38' 3}}{g\gamma_w}\right) \tag{12a}$$

$$U_{particle} = U_{current} + windweight.W.sin(Wind\ direction - \pi + \theta_w) \tag{11b}$$

$$V_{particle} = V_{current} + windweight.W.sin(Wind\ direction - \pi + \theta_w) \tag{12b}$$

where:

θ_w = Wind drift angle, this parameter relates to the Coriolis Force which influences the relative direction of wind drift vector to the wind direction, $\theta_w = \beta exp\left(\frac{\alpha|U_w|^3}{g\gamma_w}\right)$, where $\alpha = -0.3.10^{-9}$, $\beta = 28^o38'$, γ_w = Kinematic viscosity ($kg.m^{-1}s^{-1}$), and g = Specific gravity ($m.s^{-2}$).
windweight = Calibration factor for wind drag on particle

2.3. Flexible mesh for hydrodynamic model

The meshing step is the essential stage as a basis of the model domain. The mesh file was merged with bathymetry data obtained from the PUSHIDROSAL (Indonesian Navy) navigation map combined with the BIG (Geospatial Information Agency) water environment map, coastline data retrieved from Google Earth, and tidal forecasting for every boundary. The tidal prediction, employed to generate the time series of surface elevation data, was predicted based on the field measurements. We applied these tidal model data to the boundary conditions in the simulation for five boundaries (Fig. 3). We also used wind data retrieved from BMKG (Meteorological, Climatological, and Geophysical Agency of Indonesia) in the simulation in the form of hourly time series data.

2.4. Particle tracking simulation set-up.

We simulated the particle tracking model for 15 days representing the two periods of neap and spring tidal conditions. The simulation reiterated two monsoon periods: the northeast monsoon (January 1–15, 2018) and the southwest monsoon (June 10–25, 2018). Once the model had been validated, the developed model was simulated again for our ten-year study period (2018–2028) to determine the coastal accumulation of plastic debris. The model set-up is shown in Table 2.

2.4. Plastic debris flux quantification

Once the simulation achieved a normal completion status, we calculated the fluxes of plastic debris onto the coastline segments to estimate the deposition potential of plastic fragments on the coastline. This procedure could become a reference tool for regular coastal cleanup that could be applied in Banten Bay to diminish environmental degradation resulting from plastic accumulation. The debris flux calculation is determined by a formula (Liubarsetva et al., 2016):

$$f = \frac{s}{l}\left[\frac{c_2 - c_1}{t_2 - t_1}\right] \tag{13}$$

where:

f = The estimated plastic debris flux on the coastline
s = The area of coastal cell
l = The length of coastal segment
c_1 = Plastic concentration at the time t_1
c_2 = Plastic concentration at the time t_2

From Equation (13) we can determine the deposits of plastic debris by referring to the residence time of marine plastic on beach τ predicted from the field measurement. The deposits of plastic fragments can be calculated as follows:

$$d = f\tau \tag{14}$$

If the coastal cleanup period $t_{cleanup}$ is defined as the period between regular cleanups, the average deposit of plastic fragments can be calculated as:

Table 2
Hydrodynamic and Particle Tracking Model set-up applied in the simulation.

Parameter	Implemented in the simulation	
Mesh file	Digitized Bathymetry and Coastline Source: ● Indonesian Navy bathymetry map ● Water environment map established by Geospatial Information Agency of Indonesia	
Hydrodynamic Module		
Solution Technique	Shallow water equations: ● Time integration - Low order, fast algorithm ● Space discretization: Low order, fast algorithm ● Minimum time step: 0.01 sec ● Maximum time step: 3600 sec ● Critical CFL number: 0.8 Transport equations: ● Minimum time step: 0.01 sec ● Maximum time step: 3600 sec ● Critical CFL number: 0.8	
Flood and Dry	Drying depth: 0.005 m Flooding depth: 0.05 m Wetting depth: 0.1 m	
Density	Density type: Barotropic Reference temperature: 10 °C Reference salinity: 32 PSU	
Eddy viscosity	Smangorinsky formulation: 0.28 Eddy parameters: min 1.8 e^{-006} m^2/s^2, max $10^7 m^2/s^2$	
Bed resistance	Manning number: 32 [m^(1/3)/s]	
Wind forcing	Varying in time, constant in domain: BMKG daily wind data	
Boundary conditions (BC)	Tidal forecast with the coordinate as follows: BC1: 106.25058E -5.9298 S BC2: 106.22785E -5.9053 S BC3: 106.18982E -5.8858 S BC4: 106.14632E -5.8768 S BC5: 106.10313E -5.8830 S Specified level – varying in time, constant along boundary	
Particle Tracking Module		
Classes	Plastic Minimum mass 1 kg	
Sources	August simulation: Bojonegara port, plastic flux 1.4 kg/s Karangantu, plastic flux 1.4 kg/s Cibanten Estuary, plastic flux 1.4 kg/s Sunda Strait, plastic flux 2.8 kg/s	January simulation: Bojonegara port, plastic flux 2 kg/s Karangantu, plastic flux 2 kg/s Cibanten Estuary, plastic flux 2 kg/s Sunda Strait, plastic flux 4 kg/s
Decay	Exclude	
Settling	Exclude	
Erosion	Exclude	

$$d_{cleanup} = ft_{cleanup} \tag{15}$$

These approaches can be used to plan regular cleanup activities via estimations that could be used by local governments and communities.

The calculation of particle concentration within Banten Bay is limited in the northwestern boundary (near the Sunda Strait) and the northeastern boundary. This is because at those boundaries, the outflow particles are removed from the model domain, and would thus serve as an artificial coastline. Based on the particle tracking simulation, over 2018–2028, the percentage of outflowing debris was less than 10% of the total particles within the model domain. Thus, we underestimated the floating debris at those boundaries.

From the methodologies explained above, we only considered the virtual floating plastic debris particles. It should be noted that some significant states, such as the sunken plastic fragments, were neglected due to the buoyancy-loss triggered by biofouling and chemical reactions with inorganic compounds (Fazey and Ryan, 2016; Wu et al., 2020), the breaking up of micro-elements of plastic fragments (Guzzetti et al., 2018) and the ingestion by marine biota (Potocka et al., 2019; Thushari and Senevirathna, 2020). It is recommended that these issues should be investigated and quantified in future studies.

3. Results and discussion

3.1. The influence of rainfall intensity on the amount of marine debris in Banten Bay

The displacement of tidal elevation plays a role in evoking transport mechanisms within the bay. Due to the semi-enclosed nature of Banten Bay, the tidal phases (neap and spring) strongly control the current velocity variability related to astronomical forces and the monsoon-induced winds (Jithin et al., 2017). Tidal current motions may trigger a higher accumulation of marine debris during the northeast monsoon because of the higher rainfall intensity associated with it that contributes to elevated debris intake from rivers and estuaries.

Fig. 4 shows the monthly relationship between rainfall intensity and the amount of marine debris throughout 2018. Overall, the amount of rainfall-induced marine debris varied considerably. A higher amount of marine debris was observed during October to December (ranging from 0.5 to 5 kg). Rainfall intensity also peaked during the same period (ranging from 0 to 355 mm). Even though the volume of marine debris in the first week of November decreased significantly, it still had the highest value on average during the three months of the northeast monsoon. Other unsynchronized data was observed during February–March, during which the amount of marine debris declined as the sufficiently higher rainfall took place.

Statistically, the accumulation of trapped debris fragments accumulation was not generally related to precipitation events. We analyzed the linear regression for the two sets of data and identified that rainfall did not explain the variation in the weight of debris collected. Surface runoff plays a role in transport mechanisms into waterways, but only 35% of the difference in the number of total fragments collected could be explained by variations in rainfall. However, if littering rates are approximately constant over time, the first precipitation event after the dry season tends to carry more marine debris than following rainfall events (Carson et al., 2013).

Marine debris collection during the boat surveys consisted of plastic items (polyethylene terephthalate bottles, cigarettes, polyethylene packaging, plastic bags, cups/lids, footwear, and Styrofoam). Simultaneously, other fragments were of aluminum, glass, and miscellaneous items that did not include the above categories. The fragment rate of 66.35 kg per year estimated within Banten Bay could be higher due to the regular debris flows either deposited into the ocean by wind or directly accumulating in the marine environment. This value may be a significantly underestimated value because we only collected debris fragments along the path of the boat used did not fully encompass the estuary area. Moreover, low-buoyancy items such as plastic bags may have slid underneath the net and avoided capture (Lebreton et al., 2012).

3.2. Model validation

The model results were validated using currents and tidal data obtained from the previous studies (Bayhaqi et al., 2018; Wisha et al., 2015). The validation of the zonal component showed the same phase and pattern of current velocity but difference in magnitude (Fig. 5A). The negative velocity was more erratic and very low, ranging from 0 to −0.18 m/s. Moreover, the RMSE value obtained from this comparison was 14.78%. In contrast, the validation of meridional data showed a

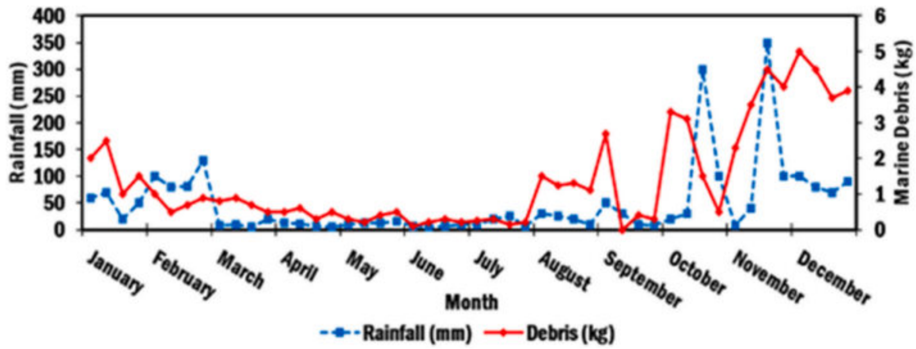

Fig. 4. The average of anthropogenic debris (red diamonds, solid lines) within Banten Bay and accumulated rainfall (blue squares, dashed lines) throughout the year of study ($R^2 = 0.35$). (For interpretation of the references to color in this figure legend, the reader is referred to the Web version of this article.)

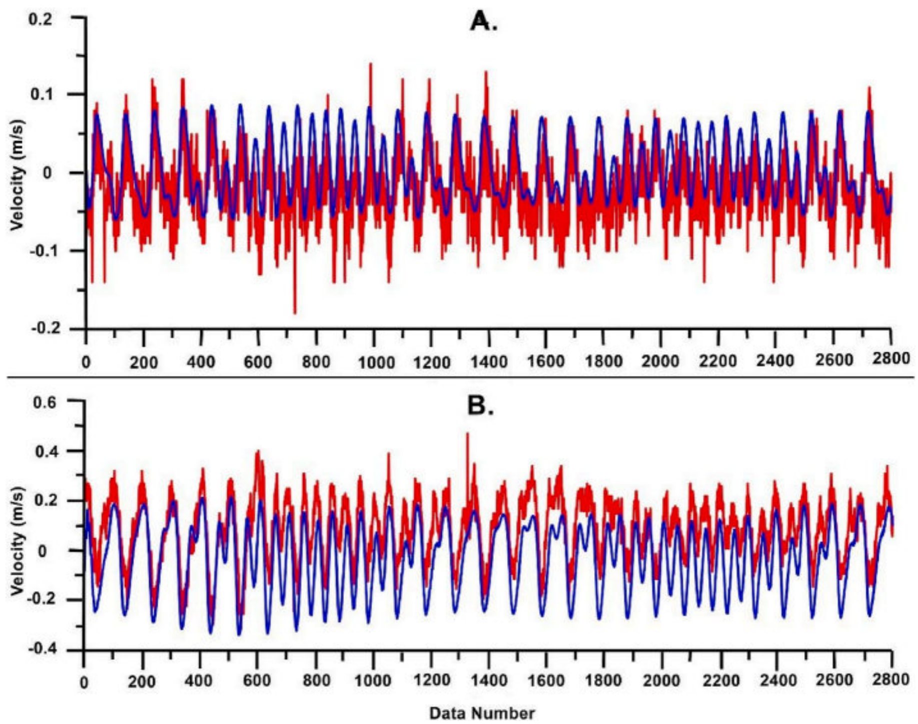

Fig. 5. Model validation of component velocity of currents. A. Zonal velocity component of current; B. Meridional velocity component of current. The blue line denotes model data, and the red line denotes field measurement data. (For interpretation of the references to color in this figure legend, the reader is referred to the Web version of this article.)

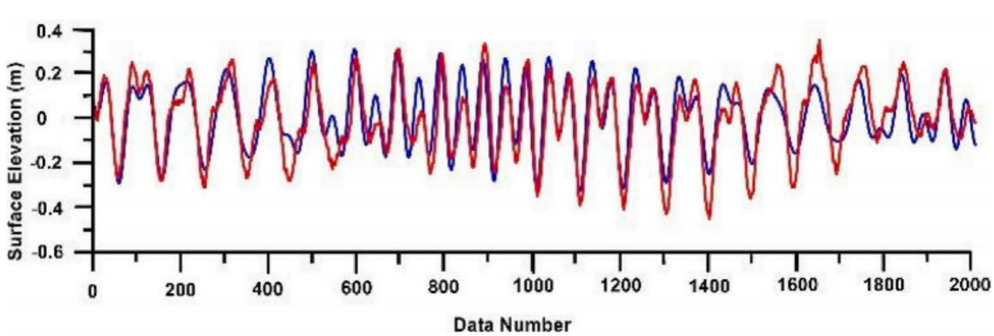

Fig. 6. Model validation of surface elevation data. The red line denotes the field measurement data while the blue line denotes the model data. (For interpretation of the references to color in this figure legend, the reader is referred to the Web version of this article.)

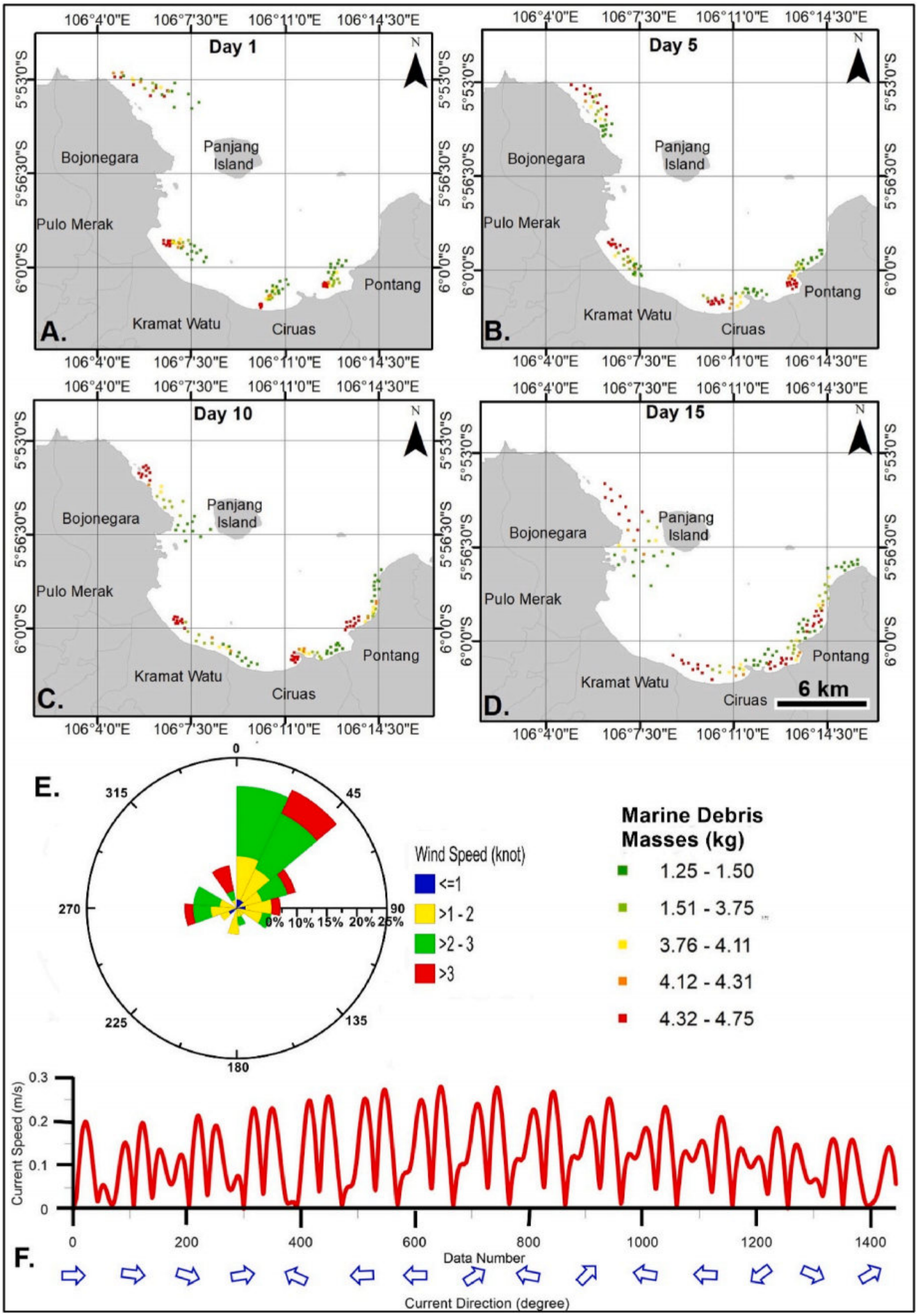

Fig. 7. Marine debris particle traces during the southwest monsoon. The particle distribution on day 1 of simulation (a); day 5 (b); day 10 (c); and day 15 (d). The wind rose diagram denotes the wind distribution during the southwest monsoon (e). The longshore current magnitudes and directions (f).

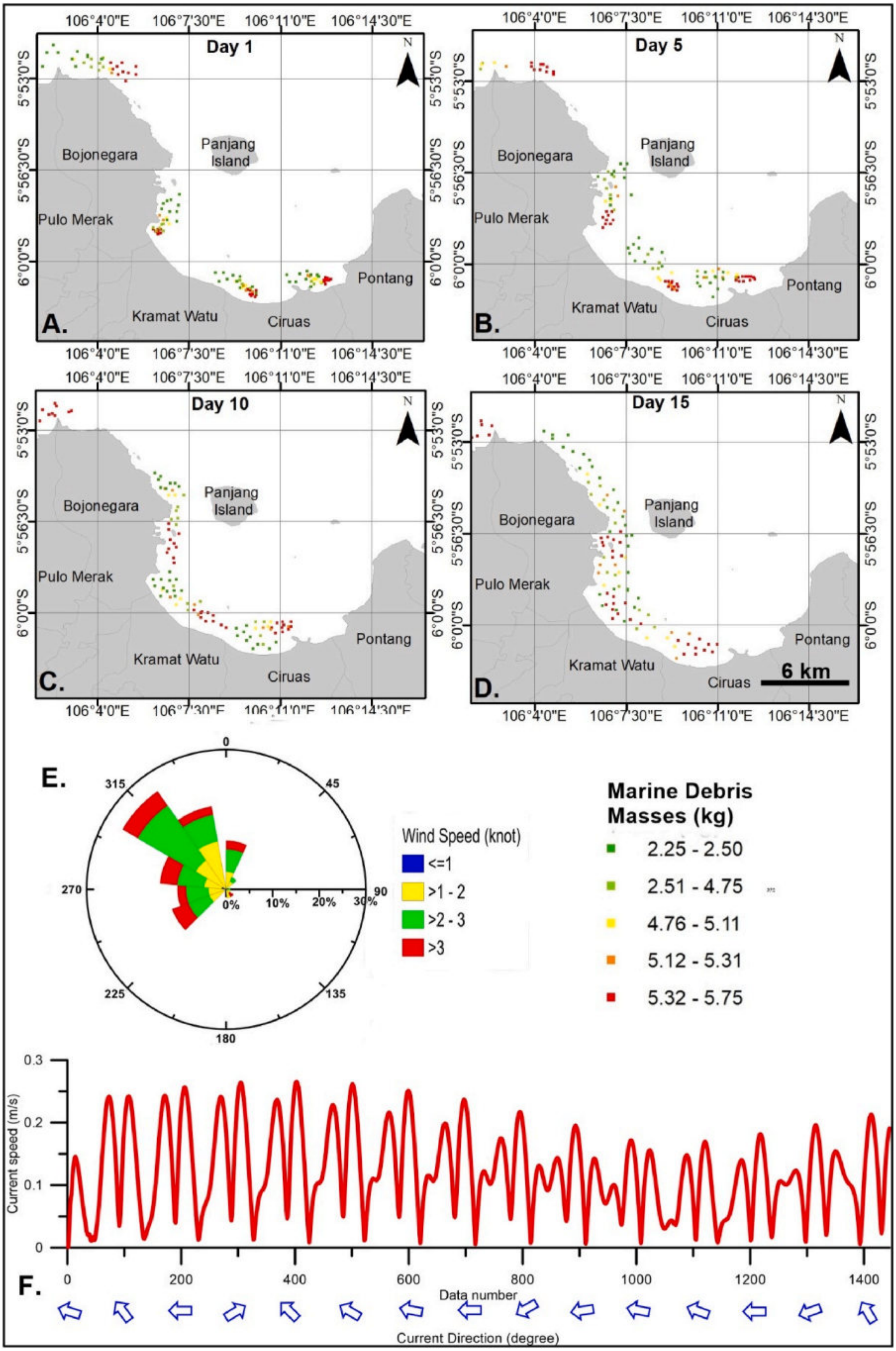

Fig. 8. Marine debris particle traces during the northeast monsoon. The particle distribution on day 1 of simulation (a); day 5 (b); day 10 (c); and day 15 (d). The wind rose diagram denotes the wind distribution during the northeast monsoon (e). The longshore current magnitudes and directions (f).

Table 3
The trace coordinates of drifters released within Banten Bay.

Location	Tidal condition	Code	Initial Coordinates	Recovery Coordinates	Main Direction	Estimated Distance (km)
Northeast monsoon survey						
Bojonegara	Ebb tides	NEM01a	106.109 E, −5.982 S	106.113 E, −5.938 S	North	7.76
Port 1	Flood tides	NEM01b		106.110 E, - 5.975 S	North	1.18
Karangantu 1	Ebb tides	NEM02a	106.165 E, −6.024 S	106.128 E, −6.010 S	West	4.55
	Flood tides	NEM02b		106.143 E, −6.016 S	West	2.65
Cibanten 1	Ebb tides	NEM03a	106.216 E, −6.014 S	106.193 E, −6.019 S	Southwest	3.59
	Flood tides	NEM03b		106.202 E, −6.014 S	West	1.75
Sunda Strait 1	Ebb tides	NEM04a	106.037 E, −5.880 S	106.016 E, −5.901 S	West	3.92
	Flood tides	NEM04b		106.021 E, −5.891 S	West	2.62
Southwest monsoon survey						
Bojonegara	Ebb tides	SW01a	106.111 E, −5.981 S	106.113 E, −6.001 S	South	5.22
Port 2	Flood tides	SW01b		106.105 E, −5.988 S	South	2.49
Karangantu 2	Ebb tides	SW02a	106.109 E, −5.981 S	106.197 E, −6.017 S	Northeast	5.21
	Flood tides	SW02b		106.178 E, −6.026 S	East	1.62
Cibanten 2	Ebb tides	SW03a	106.217 E, −6.015 S	106.236 E, −5.997 S	Northeast	3.35
	Flood tides	SW03b		106.226 E, −6.007 S	Northeast	1.47
Sunda Strait 2	Ebb tides	SW04a	106.038 E, −5.879 S	106.074 E, −5.884 S	Southeast	5.89
	Flood tides	SW04b		106.051 E, −5.879 S	Southeast	2.71

higher and more dispersed velocity than the model result, ranging from 0 to 0.45 m/s, with RMSE value of 13.48% (Fig. 5B). Zonal velocity ranged from −0.18 to 0.15 m/s, while the meridional value ranged from −0.26 to 0.5 m/s.

A plethora of errors were identified in the field measurements, proven by the asymmetry of the velocity component of current, with a significant difference in velocity fluctuation between model and field data (ranging from 0.5 to 1.25 m/s) (Fig. 5). This indicates that other external and more prominent factors play a significant role in determining current regimes. According to Johnson and Proehl (2004) and Johnson et al. (2007), near-equatorial meridional and low-frequency zonal currents are dominated by tropical instability waves with wavelengths of 1000 km and periods of 15–20 days. Sea currents with vertical shear stress and baroclinically erratic stability tend to stabilize as they move toward the equator (Wang et al., 2020). In contrast, zonal equatorial currents could be unstable, seeming more spasmodic than meridional current variability. Tidal current phases are most likely to reflect the wave influence because, during the tidal displacement phase, wave generation contributes to the characteristics of surface elevation. (Garrett and Kunze, 2007; Ondara et al., 2018; Wisha et al., 2018).

We also validated the simulation result using surface elevation data, with the RMSE of 11.89% (Fig. 6). We identified anomalies during neap tidal conditions wherein the surface elevation was 0.2 m higher than the model data. This tidal asymmetry is most likely to reflect the influence of wind-driven current in surface water that influences higher current velocity on the surface and may cause peak transport of marine debris. On the other hand, according to previous studies (Bayhaqi et al., 2018; Hoekstra et al., 2003; Wisha et al., 2015), the tidal type of Banten Bay is mixed with prevailing diurnal, and with a varying tidal range of between 20 and 90 cm.

3.3. Plastic debris traces based on flow model simulation

During the southwest monsoon, the surface wind predominantly moved northeastward at average speed of 2 knots (1.03 m/s). Higher southwesterly wind speed was identified for approximately 10% of all data (red color of wind rose in Fig. 7). Winds moved eastward and westward at specified times, affecting the longshore current profile during the simulation (bottom graph in Fig. 7). The sea currents flowed predominantly northeastward and eastward, ranging in speed from 0 to 0.28 m/s. Surface winds and currents play a significant role in triggering water mass movement that induces marine debris flow (Husrin et al., 2017). According to the simulation, plastic debris gradually moves eastward within the bay.

On day 1 of the simulation, plastic debris was released from its sources in Sunda Strait, Bojonegara Port, Karangantu, and Cibanten Estuary. The lower-mass particles (green dots) ranged from 1.25 to 1.5 kg and were easily distributed eastward by the current (Fig. 7a). The distribution pattern was slightly distorted for the Sunda Strait intake, a condition related to the higher water mass movement exiting the bay where surface wind-driven current strongly controls the surface transport mechanism. Particles with larger mass (red dots), ranging from 4.32 to 4.75 kg, tended to settle on the coastline and surface bottom, as shown by the small movements of the red dots.

On day 5 of the simulation, the movement of marine debris was generally similar to day 1. It flowed along the coastline, indicating the predominant influence of the longshore current regime (Liubartseva et al., 2016). However, we found that the plastic debris from the Sunda Strait tended to be deflected westward, moving along the coast and entering the bay past the Bojonegara Peninsula (Fig. 7b).

After ten days of simulation, the particles had overall moved further east (Fig. 7c). Plastic fragments sourced from the estuaries and Bojonegara Port showed uniform patterns, flowing parallel to the coastline. By contrast, the marine debris from Sunda Strait commenced polluting Panjang Island and entering the bay. On the final day of the simulation, the particle traces seemed more arbitrarily erratic, with particles tending to be accumulated within the eastern part of the bay (Fig. 7d). At the same time, fragments from the Sunda Strait polluted Bojonegara Port and Panjang Island in the mouth of the bay. Overall, these simulations only estimated the distribution of plastic particles for 15 days. Hence, a longer time-step simulation is likely to depict more accumulated and distributed particles according to the wind-driven current regimes within Banten Bay. The 10-year (2018–2028) simulation of particle tracking will be addressed in subsection 3.5.

In contrast to the southwest monsoon, during the northeast monsoon simulation, the southeasterly wind speed was higher, at an average of 2.05 m/s. The current magnitude ranged from 0 to 0.25 m/s and moved predominantly northeastward and northwestward. The wind and current data were correlated in the dominant direction, indicating wind-driven current regimes (Bayhaqi et al., 2018). Generally, the marine debris gradually moved northeastward during the northeast monsoon, leaving the bay.

On day 1 of the simulation (Fig. 8a), particles with a mass ranging from 2.25 to 5.75 kg were released from the four primary sources. The heavier particles (5.32–5.75 kg) tended to settle locally due to their high specific gravity. In contrast, other categories moved northwestward, strongly controlled by the stronger wind-driven current (ranging from 0.15 to 0.25 m/s) (Fig. 8).

The robust current profile observed at the beginning of the simulation affected the distribution of plastic debris. Particles moving parallel to the coastline testified to the influence of longshore current regimes in plastic debris distribution throughout the Banten coastal area. We

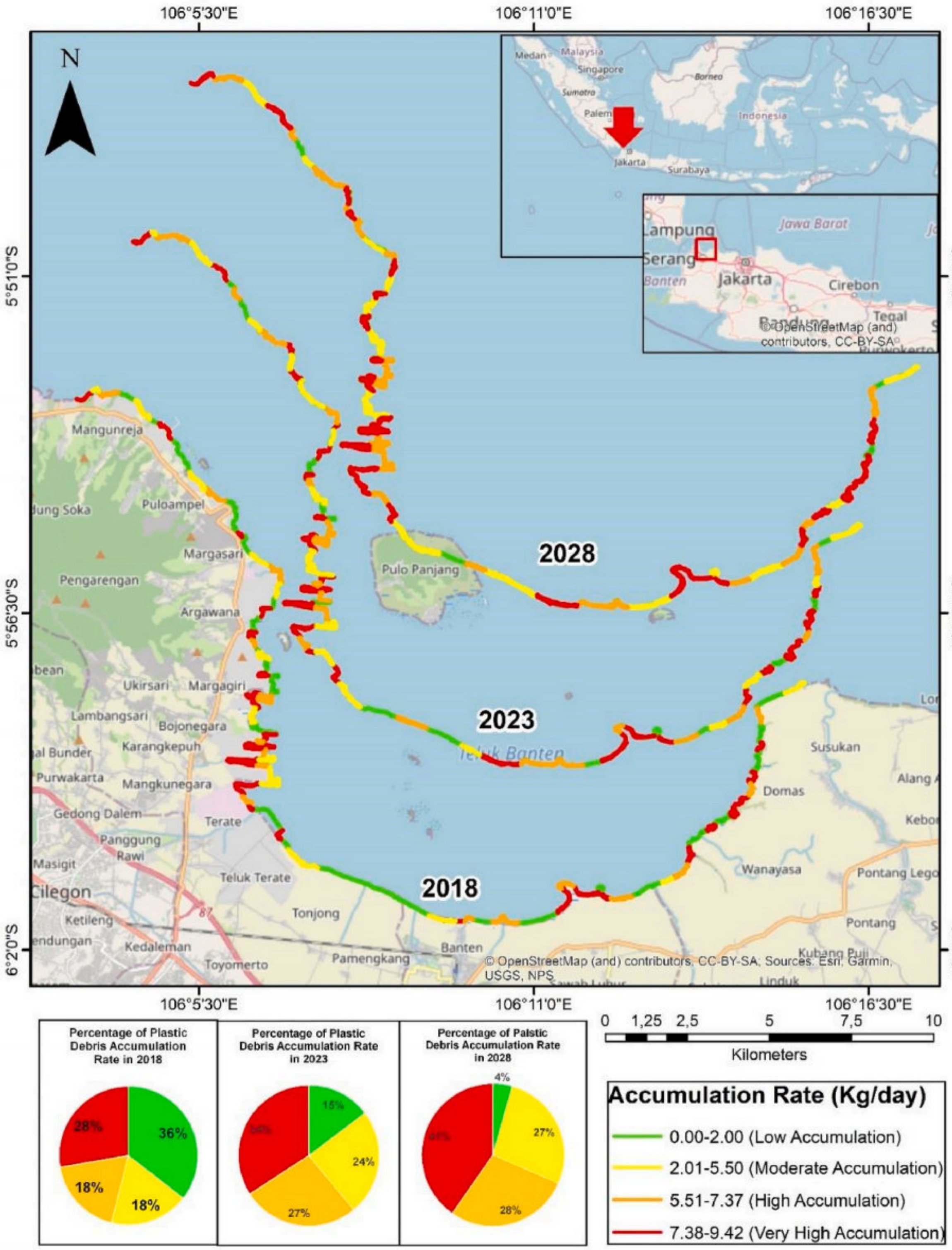

Fig. 9. The plastic debris flux prediction within Banten Bay for ten years (2018–2028).

identified a slight alteration in particle flow pattern on day 5 of the simulation (Fig. 8b). However, fragments with low masses tended to move erratically. Furthermore, particles from the Sunda Strait provenance were transported toward other areas within the Sunda Strait area (escaping the model boundary).

Conditions became more arbitrarily erratic at the two last simulations (Fig. 8c and d). The particle traces spasmodically flowed northwestward. The largest particles scattered erratically within the bay, while the lower-mass fragments tended to be transported out of the bay. Bojonegara Port and Karangantu Estuary were the areas most impacted by passing particles. Some particles may have been trapped due to the presence of coastal and port buildings. The particles from the Sunda Strait flowed southward, entering the gap between Java and Sumatra islands, under the influence of the ITF. This stronger current plays a significant role in triggering the higher movement of debris particles entering the Indian Ocean (Bayhaqi et al., 2018).

3.4. The drifter trace survey results

The wooden drifters were well-recovered locally and at distance (approximately 1.62–7.76 km from the source) (Table 3). Interestingly, for the southwest monsoon survey, tidal condition played a significant role in the inflow of marine debris. During the ebb tides, drifters released from the Sunda Strait, Bojonegara Port, and Karangantu Estuary flowed around 5 km southward and northeastward. Meanwhile, drifters from the remaining station (Cibanten Estuary) only moved around 3 km toward the northeast. By contrast, during the high tide conditions, drifter movement was not so significant, at approximately 1.7–2.6 km, because in the semi-enclosed Banten coastal bay area, current flow tended to move landward during flood tides and vice versa for low tide conditions (Bayhaqi et al., 2018; Rahmania et al., 2021). Thus, the drifters would be transported locally.

In contrast to the southwest monsoon, the drifter predominantly moved westward and northward during the northeast monsoon. At low tides, the drifters gradually flowed westward, following the coastline for 3.5–7.7 km (Table 3). In contrast, drifters from Bojonegara Port were recovered on the Bojonegara Peninsula, where extensive debris deposition induced by the ocean tides during the southwest monsoon has been previously observed (Rahmania et al., 2021). We discovered the same pattern of drifter traces during high tide condition but with shorter distances of approximately 1.1–2.6 km.

Wind-driven currents are the main factor in determining marine debris distribution (Carson et al., 2013; Lebreton et al., 2012). We discovered this relationship in Banten Bay, where the highest current speed during the southwest monsoon induced a greater distribution of plastic debris. We found that the more robust the sea−current regimes, the more distant the location reached by the drifters. These drifter survey results also revealed that local pollutants would be retained and circulated around Banten Bay, resulting in local debris accumulation and possibly threatening other affected areas.

3.5. Estimation of accumulated plastic debris over the ten-year of simulation

Based on the model simulation, it is estimated that in 2018, 36% of the 45 km coastline of the study area was in the low accumulation category of plastic debris (ranging from 0 to 2 kg/day), with this category scattered across the middle to northern part of the bay. The moderate and high accumulation categories each composed 18% of the study area. The remaining 28% was in the very high accumulation category, with a maximum rate of 9.42 kg/day (Fig. 9). Furthermore, the area threatened by overwhelming accumulation of plastic waste was found to be concentrated in the areas surrounding Cibanten Estuary and Bojonegara Port.

We predicted that the menace of debris accumulation in the coastal area of Banten Bay will increase in 2023, with the exceptionally high, high, and moderate accumulation categories increasing to 34%, 27%, and 24%, respectively (Fig. 9). In contrast, the low accumulation area will significantly decline by one-half from the 2018 coverage. Extreme debris accumulation is predicted to occur in 2028 if no mitigation efforts are applied. Almost 41% of the coastal area of Banten Bay will be covered by plastic and other solid wastes, as denoted by the red line in Fig. 9. We estimated that the debris-free area would periodically decrease to 4% of the low accumulation area. However, the high and moderate categories seem stable and equal, comprising less than 30% of debris cover.

Over time, exceptionally high debris accumulation (ranging from 7.38 to 9.42 kg/day) will become the majority situation throughout the coastline of Banten Bay, with the most threatened regions being in the eastern and western parts of the bay. This situation reflects the seasonal dominance in movement of plastic debris predominantly eastward and westward during the southwest and northeast monsoons, respectively. Thus, the accumulation area of floating plastic debris may be in the areas near to Bojonegara and Cibanten. As well as its negative impact, this accumulation of debris in the coastal zone could cause other environmental and health problems (Husrin et al., 2017).

The rapid urban development taking place in the coastal area of Banten Bay is creating significant environmental impacts related to the increase in anthropogenic wastes (Rahmania et al., 2021) and immediate actions are therefore crucial to protect the coastal area from solid waste and plastic debris pollution. According to a simple tabulation, if there is no cleanup during the simulation period, Banten Bay's annual plastic debris accumulation will be approximately 27.34 tons/km. We recommend that a coastal cleanup should be conducted every ten days, resulting in the average plastic debris deposits of approximately 759 kg/km in each period between cleanups.

4. Conclusion

The distribution of plastic debris relies on the dominant direction of wind-driven currents and the thresholds of rainfall intensity. Higher marine debris intake in the estuaries occurs during the northeast monsoon, during which the more significant river discharge probably brings the peak abundance of debris. During the northeast monsoon, the particle tracks tend to move westward and northward within the bay and vice versa for the southwest monsoon. These oscillations induced marine debris accumulation in several areas within and outside Banten Bay. Local pollutants sourced from the very dense settlement around estuaries will be retained and circulating in coastal regions and in the mouth of bay, inducing local debris accumulation and threatening nearby areas. The accumulation of plastic debris is expected to worsen if no mitigation efforts are applied to control the coastal zone's solid and plastic waste deposits. A coastal cleanup every ten days to manage debris deposit is recommended.

Author contributions

Ulung J. Wisha: Conceptualization, Methodology, Software, Visualization, Validation, Formal analysis, Resources, Writing-Original Draft preparation, Writing-Review & Editing, Supervision, Project administration, and Funding Acquisition. **Wisnu A. Gemilang & Yusuf J. Wijaya:** Conceptualization, Software, validation, Investigation, Methodology, Project administration. **Anang D. Purwanto:** Conceptualization, Methodology, Writing-Review & Editing. All authors have read and agreed to the published version of the manuscript.

Declaration of competing interest

The authors declare that they have no known competing financial interests or personal relationships that could have appeared to influence the work reported in this paper.

Acknowledgement

Acknowledgments are given to Research Institute for Coastal Resources and Vulnerability (RICRV) – Ministry of Marine Affairs and Fisheries (MMAF) for the research funding in 2018 with a grant number of 2428.003.001.053B, to the Head of RICRV, to the data providers and to those who contribute to the process of field survey.

References

Bayhaqi, A., Wisha, U.J., Surinati, D., 2018. Modeling tidal current on banten bay during transitional monsoons. Jurnal Segara 14 (2), 95–105. https://doi.org/10.15578/segara.v14i2.6452.

Bayram, M., Partal, T., Orucova Buyukoz, G., 2018. Numerical methods for simulation of stochastic differential equations. Adv. Differ. Equ. (1) https://doi.org/10.1186/s13662-018-1466-5, 2018.

Carson, H.S., Lamson, M.R., Nakashima, D., Toloumu, D., Hafner, J., Maximenko, N., McDermid, K.J., 2013. Tracking the sources and sinks of local marine debris in Hawai'i. Mar. Environ. Res. 84 https://doi.org/10.1016/j.marenvres.2012.12.002.

Fazey, F.M.C., Ryan, P.G., 2016. Biofouling on buoyant marine plastics: an experimental study into the effect of size on surface longevity. Environ. Pollut. 210 https://doi.org/10.1016/j.envpol.2016.01.026.

Garrett, C., Kunze, E., 2007. Internal tide generation in the deep ocean. Annu. Rev. Fluid Mech. 39, 57–87. https://doi.org/10.1146/annurev.fluid.39.050905.110227.

Guzzetti, E., Sureda, A., Tejada, S., Faggio, C., 2018. Microplastic in marine organism: environmental and toxicological effects. In: Environmental Toxicology and Pharmacology, 64. https://doi.org/10.1016/j.etap.2018.10.009.

Hoekstra, P., Lindeboom, H., Bak, R., Bergh, G. van den, Tiwi, D.A., Douven, W., Heun, J., Hobma, T., Hoitink, T., Kiswara, W., Meesters, E., Noor, Y., Sukmantalya, N., Nuraini, S., Weering, T. van, 2003. Teluk banten research programme: an integrated coastal zone management study. In: Levelt, W.J.M. (Ed.), Scientific Programme Indonesia-Netherlands. Koninklijke Nederlandse Akademie van Wetenschappen, pp. 59–70.

Husrin, S., Wisha, U.J., Prasetyo, R., Putra, A., Attamimi, A., 2017. Characteristics of marine litters in the west coast of bali. Jurnal Segara 13 (2). https://doi.org/10.15578/segara.v13i2.6449.

Inniss, L., Simcock, A., 2017. The first global integrated marine assessment: world ocean assessment i. In: The First Global Integrated Marine Assessment: World Ocean Assessment I. https://doi.org/10.1017/9781108186148.

Jithin, A.K., Unnikrishnan, A.S., Fernando, V., Subeesh, M.P., Fernandes, R., Khalap, S., Narayan, S., Agarvadekar, Y., Gaonkar, M., Tari, P., Kankonkar, A., Vernekar, S., 2017. Observed tidal currents on the continental shelf off the east coast of India. Continent. Shelf Res. 141 https://doi.org/10.1016/j.csr.2017.04.001.

Johnson, E.S., Bonjean, F., Lagerloef, G.S.E., Gunn, J.T., Mitchum, G.T., 2007. Validation and error analysis of OSCAR sea surface currents. J. Atmos. Ocean. Technol. 24 (4) https://doi.org/10.1175/JTECH1971.1.

Johnson, E.S., Proehl, J.A., 2004. Tropical instability wave variability in the Pacific and its relation to large-scale currents. J. Phys. Oceanogr. 34 (10). https://doi.org/10.1175/1520-0485(2004)034<2121:TIWVIT>2.0.CO;2.

Lebreton, L.C.M., Greer, S.D., Borrero, J.C., 2012. Numerical modelling of floating debris in the world's oceans. Mar. Pollut. Bull. 64 (3) https://doi.org/10.1016/j.marpolbul.2011.10.027.

Liubartseva, S., Coppini, G., Lecci, R., Creti, S., 2016. Regional approach to modeling the transport of floating plastic debris in the Adriatic Sea. Mar. Pollut. Bull. 103 (1–2) https://doi.org/10.1016/j.marpolbul.2015.12.031.

Maharani, A., Purba, N.P., Faizal, I., 2018. Occurrence of beach debris in tunda island, banten, Indonesia. E3S Web of Conferences 47. https://doi.org/10.1051/e3sconf/20184704006.

Mahbub, A., 2018. Bangkai Paus Sperma Sepanjang 9 meter terdampar di Wakatobi (9-meter Sperm Whale carcass Stranded in Wakatobi). Tempo Online Magazine, 114972. https://tekno.tempo.co/read/1147972/bangkai-paus-sperma-sepanjang-9-meter-terdampar-di-wakatobi (in Indonesian).

Miladinova, S., Macias, D., Stips, A., Garcia-Gorriz, E., 2020. Identifying distribution and accumulation patterns of floating marine debris in the Black Sea. Mar. Pollut. Bull. 153 https://doi.org/10.1016/j.marpolbul.2020.110964.

Neumann, D., Callies, U., Matthies, M., 2014. Marine litter ensemble transport simulations in the southern North Sea. Mar. Pollut. Bull. 86 (1–2) https://doi.org/10.1016/j.marpolbul.2014.07.016.

North, E.W., Schlag, Z., Hood, R.R., Li, M., Zhong, L., Gross, T., Kennedy, V.S., 2008. Vertical swimming behavior influences the dispersal of simulated oyster larvae in a coupled particle-tracking and hydrodynamic model of Chesapeake Bay. Mar. Ecol. Prog. Ser. 359 https://doi.org/10.3354/meps07317.

Ondara, K., Rahmawan, G.A., Gemilang, W.A., Wisha, U.J., Dhiauddin, R., 2018. Numerical hydrodynamic wave modelling using spatial discretization in Brebes waters, Central Java, Indonesia. Int. J. Adv. Sci. Eng. Inf. Technol. 8 (1) https://doi.org/10.18517/ijaseit.8.1.4166.

Ouellette, N.T., Xu, H., Bodenschatz, E., 2006. A quantitative study of three-dimensional Lagrangian particle tracking algorithms. Exp. Fluid 40 (2). https://doi.org/10.1007/s00348-005-0068-7.

Potemra, J.T., 2012. Numerical modeling with application to tracking marine debris. Mar. Pollut. Bull. 65 (1–3) https://doi.org/10.1016/j.marpolbul.2011.06.026.

Potocka, M., Bayer, R.C., Potocki, M., 2019. Plastic pollution affects American lobsters, Homarus americanus. Mar. Pollut. Bull. 138 https://doi.org/10.1016/j.marpolbul.2018.12.017.

Purba, N.P., Handyman, D.I.W., Pribadi, T.D., Syakti, A.D., Pranowo, W.S., Harvey, A., Ihsan, Y.N., 2019. Marine debris in Indonesia: a review of research and status. Mar. Pollut. Bull. 146, 134–144. https://doi.org/10.1016/j.marpolbul.2019.05.057.

Rahmania, R., Setiawan, A., Tussadiah, A., Kusumaningrum, P.D., Yulius Prihantono, J., Gautama, B.G., Pranowo, W.S., Aisyah Nugraha, A.W., Gusmawati, N.F., Widjanarko, E., Arifin, T., 2021. Mapping seasonal marine debris patterns and potential hotspots in Banten Bay, Indonesia. IOP Conf. Ser. Earth Environ. Sci. 763 (1) https://doi.org/10.1088/1755-1315/763/1/012056.

Rifa'i, B., 2018. Sampah Berceceran di Teluk Banten Dari Kasur hingga Plastik (Scattered Garbage in Banten Bay Consists of Mattreses and Plastics). Detik.Com. https://news.detik.com/berita/d-4317855/sampah-berceceran-di-teluk-banten-dari-kasur-hingga-plastik.

Silva, M. L. da, Sales, A.S., Martins, S., Castro, R. de O., Araújo, F.V.de, 2016. The influence of the intensity of use, rainfall and location in the amount of marine debris in four beaches in Niteroi, Brazil: sossego, Camboinhas, Charitas and Flechas. Mar. Pollut. Bull. 113 (1–2) https://doi.org/10.1016/j.marpolbul.2016.10.061.

Susanto, R.D., Wei, Z., Adi, T.R., Zheng, Q., Fang, G., Fan, B., Supangat, A., Agustiadi, T., Li, S., Trenggono, M., Setiawan, A., 2016. Oceanography surrounding krakatau volcano in the Sunda Strait, Indonesia. Oceanography 29 (2). https://doi.org/10.5670/oceanog.2016.31.

Thushari, G.G.N., Senevirathna, J.D.M., 2020. Plastic pollution in the marine environment. Heliyon 6 (Issue 8). https://doi.org/10.1016/j.heliyon.2020.e04709.

Van Sebille, E., England, M.H., Froyland, G., 2012. Origin, dynamics and evolution of ocean garbage patches from observed surface drifters. Environ. Res. Lett. 7 (4) https://doi.org/10.1088/1748-9326/7/4/044040.

Wang, F., Feng, J., Wang, Q., Zhang, L., Hu, S., Hu, D., 2020. Instability in boundary layer between the North Equatorial Current and underlying zonal jets based on mooring observations. J. Oceanol. Limnol. 38 (5) https://doi.org/10.1007/s00343-020-0015-8.

Werner, S., Budziak, A., Van Franeker, J.A., Galgani, F., Hanke, G., Maes, T., Mattidi, M., Nilsson, P., Oosterbaan, L., Priestland, E., Thompson, R., Veiga, J.M., Vlachogianni, T., 2016. Harm Caused by Marine Litter - Thematic Report. JRC Technical Report.

Wisha, U.J., Husrin, S., Prihantono, J., 2015. Hidrodinamika perairan teluk banten pada musim peralihan (Agustus–September). Indone. J. Mar. Sci. 20 (2), 101–112. https://doi.org/10.14710/ik.ijms.20.2.101-112 (in Indonesian).

Wisha, U.J., Tanto, T.A., Pranowo, W.S., Husrin, S., 2018. Current movement in Benoa Bay water, Bali, Indonesia: pattern of tidal current changes simulated for the condition before, during, and after reclamation. Reg. Stud. Mar. Sci. 18, 177–187. https://doi.org/10.1016/j.rsma.2017.10.006.

Wu, N., Zhang, Y., Li, W., Wang, J., Zhang, X., He, J., Li, J., Ma, Y., Niu, Z., 2020. Co-effects of biofouling and inorganic matters increased the density of environmental microplastics in the sediments of Bohai Bay coast. Sci. Total Environ. 717 https://doi.org/10.1016/j.scitotenv.2019.134431.

Zhao, D.H., Shen, H.W., Tabios, G.Q., Lai, J.S., Tan, W.Y., 1994. Finite-volume two-dimensional unsteady-flow model for river basins. J. Hydraul. Eng. 120 (7) https://doi.org/10.1061/(asce)0733-9429(1994)120:7(863).